

Development of Large Expansion Hydroforming Technology Achieving Three-times Expanding

Manabu WADA*
Keinosuke IGUCHI

Masaaki MIZUMURA
Hiromitsu KANEDA

Abstract

Tube hydroforming (hereinafter referred to as “HF”) is useful for the integrated forming of hollow parts, the expansion degree of which is approximately 1.0 times and 1.4 times the cross-sectional length of the blank tube at maximum. We studied large expansion technology of HF in order to target a broad range of applications of HF and found that by coupling the technologies of “multi-process unidirectional expansion” and “intersectional movable die technology”, it is possible to expand the circumference of a blank tube by a factor of three without intermediate heat treatment. Additionally, integrated the axel housings, of which only the middle part is expanded, achieving about 10% weight reduction.

1. Introduction

Hydroforming (hereinafter referred to as “HF”) is a processing method wherein a tube is placed within dies and clamped by the dies, the inside of the tube being filled with water and then expanded by an internal pressure applied (hereinafter referred to as “expansion”) and the tube wall being fitted to the configuration of the dies. In Fig. 1, the general process of HF is shown. The characteristic feature of HF is that the thickness reduction at the expansion part is suppressed as the tube ends are pushed inward along the axial direction by the axial feeding punches (hereinafter referred to as “axial feeding”) together with the application of an internal pressure at the time of expansion.¹⁻³⁾ One of the indicators that shows the extent of expansion in HF is the expansion ratio. The expansion ratio η is defined as below when the circumferential length of the section after expansion is expressed as L_1 and that of the blank tube is expressed as L_0

$$\eta = L_1 / L_0$$

HF is a process that has high merits in integrated forming of hollow parts of automobiles and weight reduction of such parts. However, the expansion ratio of the past HF technology is about 1.0–1.1, and approximately 1.4 at the highest (Fig. 2).⁴⁾ Therefore, application of HF to automobile parts has been partial and limited only to parts such as the cross member and side member of a chassis system, the exhaust manifold of the gas exhaust system, etc. To overcome this limitation and enjoy the several merits of integrated forming of hollow parts and weight reduction by widening out the appli-

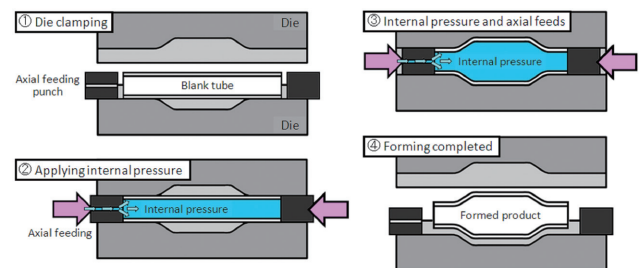


Fig. 1 Schematics of conventional hydroforming process flow

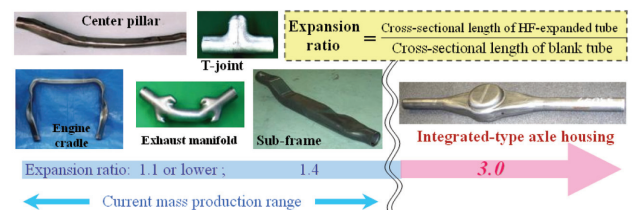


Fig. 2 Expansion ratios of hydroforming and applied products

cation of HF, the development of HF technologies that enable large expansion by enhancing formability limit has become important.

Although there are examples where large expansion by HF coupled with intermediate heat treatment and pipe-end diameter-reduc-

* Researcher, Dr.Eng., Nagoya R&D Lab.
5-3 Tokaimachi, Tokai City, Aichi Pref. 476-8686

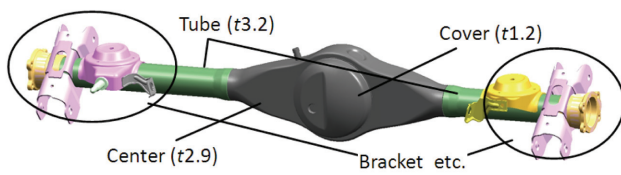


Fig. 3 Schematic of banjo-type axle housing

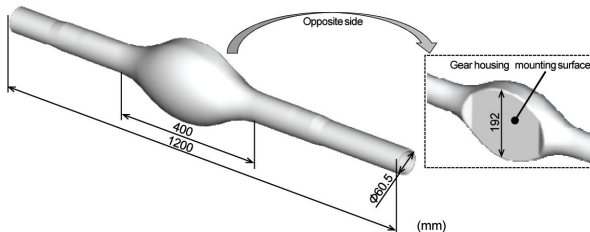


Fig. 4 Integrated axle-housing with a 3D curved shape

ing process was realized.⁵⁾ However, cold forming, i.e., HF without any intermediate heat treatment, is desirable when mass production is considered. Then authors came to tackle the development of “large expansion hydroforming technology,” aiming at the expansion ratio $\eta = 3.0$ using HF technology that consists of only cold forming without intermediate heat treatment.

Furthermore, axle housing is one of the important part of automobiles related to safety. This is a hollow suspension part that incorporates differential gears, a drive shaft, differential gear oil, etc. There are two types of axle housing, banjo-type and split-type; the banjo-type housing is widely employed owing to the ease of attaching and detaching of differential gears and simplicity in structure.⁶⁾ Since the current banjo-type axle housing (Fig. 3) comprises pluralities of press-formed subparts which are welded together; therefore, elimination of welded subparts improves the fatigue durability in addition to bringing about a weight reduction.

However, for the fabrication of an integrated single-piece type axle housing, expansion technology having large expansion ratio, reaching as high as 3, is needed as the fabrication of such parts by the conventional HF process is difficult. Sufficient inward material flow can not be obtained by the axial feeding punch alone for such parts, which have a bulge in the center of a long pipe. The authors, therefore, took up the challenge of fabricating integrated one-piece type banjo-type axle housing and the weight-reduction to be realized thereby. Since HF for the fabrication of the integrated one-piece type is able to realize the axle configuration that the conventional press-forming process is unable to realize, three-dimensional curved configurations, advantageous for fatigue durability characteristics and noise-vibration characteristics, have been employed for axle housing (Fig. 4).

Herein, authors report the outline of the large expansion hydroforming technology that they have developed and the result of the trial-base fabrication of integrated one-piece type axle housing employing this technology.

2. Outline of Large Expansion Hydroforming Technology

2.1 Multi-process unidirectional expansion

To realize large expansion by HF, the possibility of positive employment of pure shearing deformation that enables expansion while suppressing the thickness reduction has been studied. In HF, expan-

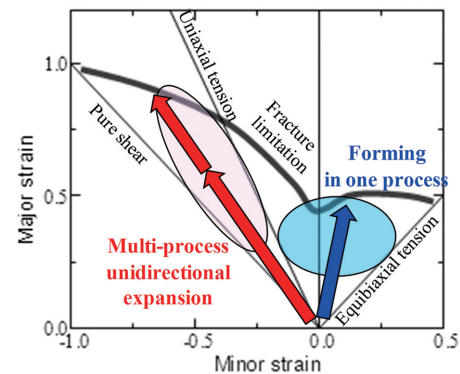


Fig. 5 Comparison between forming in one process and multi-process unidirectional expansion under all circumferences expanding

sion in the state of pure shearing deformation is made possible by applying sufficient axial feeding; however, sufficient axial feeding cannot be always obtained as excessive axial feeding causes buckling. For instance, in the case of formation of free bulging where the entire circumference of a section is expanded, when axial feeding is applied, buckling takes place very soon, the expansion part having failed to reach the state of pure shearing deformation. Axial feeding without buckling is only limited to the state of uniaxial tension that exists in circumferential direction,⁷⁾ accordingly large expansion is difficult.

Clamping of the blank tube with dies is effective to suppress buckling. For example, if the expansion is limited to only one direction, buckling is less likely to take place, even if the extent of clamping of the material by the dies is increased and axial feeding is increased. Consequently, forming in the state of pure shearing rather than in the state of uniaxial tension becomes possible⁸⁾ and the possibility of realization of larger expansion grows (Fig. 5). Thus, multi-process unidirectional expansion method has been developed. This is a process wherein expansion is performed by limiting the direction of expansion, and large expansion is realized by repeating the expansion process in multiple steps.⁹⁾

2.2 Intersectional movable die technology

Forming difficulty is high in HF when expanding only the center part of a long tube, similar to the case of axle housing, because the material cannot easily flow into the expansion part owing to frictional resistance between the material and the dies, even if axial feeding is applied at the tube ends. Therefore forming becomes difficult as the deformation is either caused by two dimensional tension or equibiaxial tension, both of which provide very low fracture limitation (Fig. 6 (1)). One of the countermeasures for such cases is the moving die technology¹⁰⁾ that separates the material-contacting part of the die from the main die and moves it simultaneously with axial feeding applied at the tube ends. With this technology, axial feeding as far as to the center part of a long tube becomes possible without being affected by the frictional resistance and expansion in the state of pure shearing deformation becomes possible, thereby realizing large expansion. However, its application is limited only to the case where the expanded height from the center line of the tube is small, like that of the branch tube formed in such a manner.

In this development, where large expansion (with the expansion ratio of 3.0) is desired, to-be-expanded part becomes essentially long along the axial direction. Herein, even if axial feeding is directly applied to the to-be-expanded part using movable dies, since the dies cannot clamp the blank tube entirely in the early stage of ex-

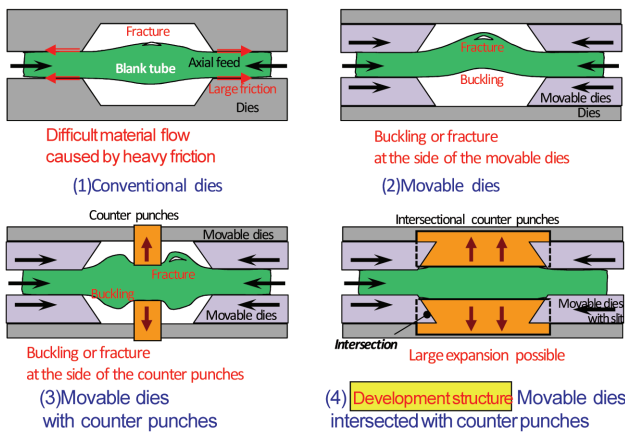


Fig. 6 Dies structure and formability

pansion, either buckling may take place at the unclamped part when the axial feeding precedes, or fracture may take place when the internal pressure precedes (Fig. 6 (2)). A countermeasure conceivable for this is a method of suppressing the buckling by installing counterpunches on the to-be-expanded part, thus increasing the clamped zone length by the counterpunches. However, since counterpunches have to be installed so that they do not interfere with the movable dies, a gap between the movable dies and the counterpunches inevitably required at the early stage of expansion and either buckling or fracture is caused there (Fig. 6 (3)).

Thereafter, the intersectional movable die structure using movable dies with a slit and intersectional counterpunches have been developed. In this process, counterpunches can clamp the entire to-be-expanded part from the early stage of expansion work and also the movable dies can move forward (Fig. 6 (4)).⁹⁾

2.3 Outline of the expanding process

The abovementioned “large expansion hydroforming technology” was developed by coupling the aforementioned “multi-process unidirectional expansion technology” and the “intersectional movable die technology” and was applied to the formation of an integrated single-piece type axle housing.

The entire forming process comprises three HF processes (Fig. 7). A tube of external diameter of $D = 60.5$ mm, wall thickness $t = 2.8$ mm, length $L = 1640$ mm, and of steel quality of STKM11A was used as the blank tube. The expansion ratio η is 2.8.

In the first process (HF1), the blank tube is expanded along upward and downward directions by means of the intersectional movable die technology. In this process, an internal pressure is applied to the blank tube after clamping the blank tube and then axial feedings are provided by axial feeding punches to the blank tube and the movable dies with slits installed inside the stationary dies. At this very moment of processing when the blank tube begins to be expanded upward and downward, intersectional counterpunches also move upward and downward. The entire structure of the movable dies with the slit and the intersectional counterpunches is designed in such a way so that it does not interfere with each other. Details will be introduced in the next chapter. The movable dies with slit are position-controlled and the counterpunches are load-controlled at a constant load.

In the second process (HF2), the blank tube is expanded in forward direction and rearward directions by the conventional moving dies. However, unlike HF1, the movable dies and counterpunches do not intersect.

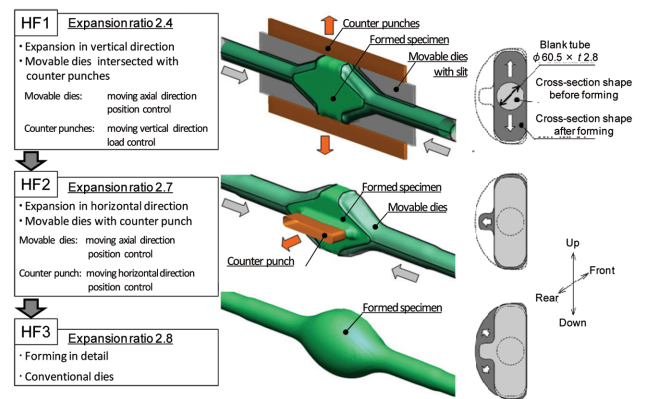


Fig. 7 Forming process of integrated axle housing using large expansion hydroforming technology

In the third process (HF3), conventional stationary dies, separable with the upper and lower die, were used to obtain exact configuration by applying a high pressure.

3. Study on Details of the First Hydroforming Process

3.1 Structure of intersectional movable dies

In the intersectional movable die technology, movable dies with slits and intersectional counterpunches (hereinafter referred to as “counter”) are used, and the loading path on three axes of the axial feeding, internal pressure, and counter load greatly influences formability. Thereafter, out of all three forming processes mentioned above for integrated one-piece type axle housing, influence of the forming condition on formability was studied through numerical analysis and experiments so as to form a shape similar to the actual shape formed in the first process (HF1), where the intersectional movable die technology was employed.¹¹⁾

Basic dimensions and approximate figures of the blank tube and the formed sample are shown in Fig. 8. A tube of external diameter $D = 60.5$ mm, wall thickness $t = 2.5$ mm, length $L = 1570$ mm, and of steel quality of STKM11A was used as the blank tube. The formed sample has a configuration of only a bulge expanded at the center part of the blank tube and the dimensions of the maximum expansion part was set with a width of expansion of $W = 185$ mm, length of expansion of $L_E = 120$ mm, and thickness of expansion $H = 70$ mm. Expansion ratio η is approximately 2.6.

The entire die structure comprises upper and lower stationary dies, four movable dies with slits installed on the upper and lower sides of the left and right stationary dies, and two counters, each of which were installed on the upper- and lower-side of the stationary dies, respectively (Fig. 9). Movable dies with slits are provided with grooves corresponding to the shape of the counter, and its forward travel without interference with counters is possible.

Next, forming procedure is explained. A schematic layout of the dies together with the profile of tube before and after forming is shown in Fig. 9. In the first place, the blank tube is placed on the lower movable dies with slits each being located at the backward stroke end position and the counters being located at each forward stroke end position. Then, the whole set of upper dies is lowered and it clamps the blank tube. Then, the blank tube is filled in with forming water with each tube end being sealed with the axial feeding punch. Thereafter, a constant load F is applied onto the counters and the internal pressure p is applied along the loading path, as will be described later. Each axial feeding punch and movable dies with

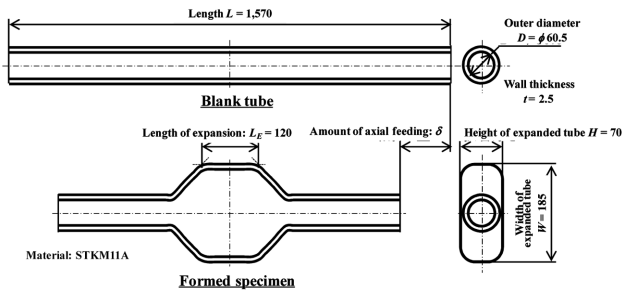


Fig. 8 Sizes and shapes of blank tube and specimen

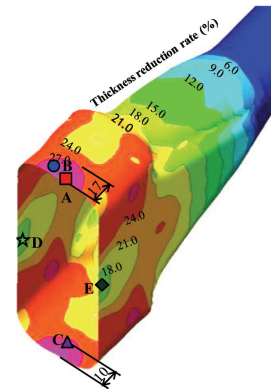


Fig. 10 Thickness distribution after forming

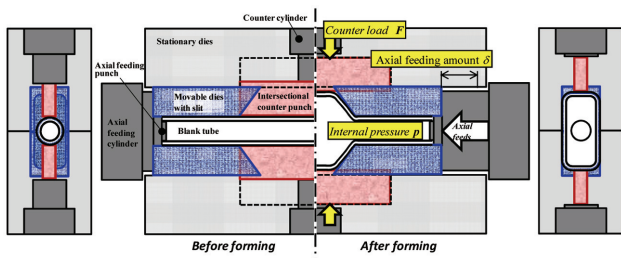


Fig. 9 Structure of intersectional movable dies before and after forming

slits are simultaneously pushed forward by the axial feeding amount of δ , under the internal pressure p . Axial feeding punches and the movable dies with slits were position-controlled, internal pressure was pressure-controlled, and counters were load-controlled at a constant load. Furthermore, the counter load F was set to allow the counter to be slowly pushed backward, making a gradual backward movement in accordance with the progress of forming. At the end, the blank tube is sufficiently expanded and each movable die moves to its forward stroke end and each counter to its backward stroke end. Finally, the internal pressure and the counter load are relieved and then the formed sample is taken out, thus completing the process of forming.

3.2 FEM analysis method

In the first place, the forming possibility of large expansion HF by means of intersectional movable die technology was studied.¹¹⁾ Numerical analysis was used for determining optimum loading path and for predicting the forming condition. For FEM solver, PAM-STAMP of explicit method was used and analysis was made on shell elements. Coefficient of friction μ was taken as $\mu = 0.09$, taking into consideration the use of a lubricant.

An analysis result of thickness distribution after forming along the optimum loading path is shown in Fig. 10, where the axial feeding amount δ is 132 mm, maximum internal pressure p is 37 MPa and counter load F is 38 kN. From the analysis, assuming that the fracture limit is at the thickness reduction ratio of 40%, maximum ratio of thickness reduction was found to be 31% at A in the figure, thus the possibility of forming was obtained. In addition, thickness reduction is remarkable in the neighborhood of A, B, and C on the most expanded side, and small in the neighborhood of D and E on the flat planes.

Next, strain condition after forming at all elements in the analysis model, strain path of A–E, and the estimated fracture limitation are shown in Fig. 11. It is confirmed that the strain condition of all elements stays between pure shearing and uniaxial tension states. It is considered that even in this shape where only the center part of a long tube is bulged, forming could be performed in the strain condi-

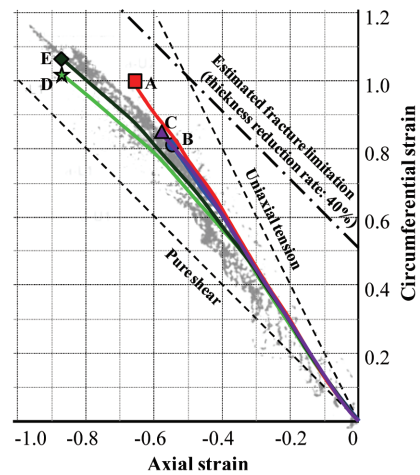


Fig. 11 Strain conditions and strain paths

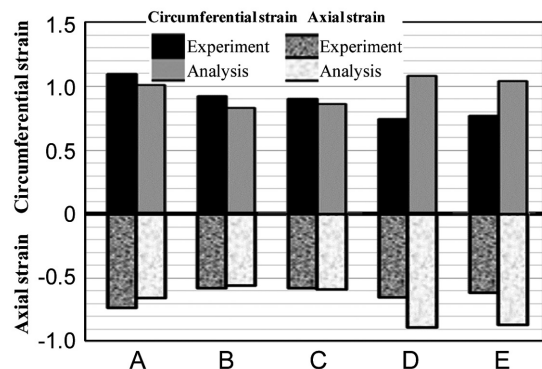


Fig. 12 Comparison of axial strain and circumferential strain between experiment and analysis

tion of being between pure shearing state having high formability limit and uniaxial tension state by employing the movable dies with slits. Furthermore, it is known that A, B, and C are near to the fracture limitation line, indicating the progress of thickness reduction.

To verify the appropriateness of the numerical analysis, scribed circles of 5 mm in diameter were transcribed on the blank tube and the experiment was conducted. Then, strain was measured after forming and compared with the analysis result. Comparison of strain conditions of A–E is shown in Fig. 12. Analysis results at A, B, and

C show approximate agreement with the experiment result, however, strains obtained by the experiment at D and E were smaller than those of the analysis result.

One of the reasons considered is the effect of lubrication. In the neighborhoods of D and E, the blank tube slides on the stationary die for a considerable distance, and there's a possibility of lack of lubrication in the experiment. Namely, it is presumed that in the experiment, the frictional resistance grew higher locally than that of the one in analysis and thereby deformation in the neighborhoods of D and E was suppressed. For movable dies, it is considered that the influence of lubrication on formability is smaller as the straight part of the blank tube and the dies travel together with each other,¹⁰⁾ however, it is also considered that the surface area of the stationary dies on which the expansion part slides is large in this forming; therefore, difference in lubricating condition influenced the formability. On the other hand, the strain conditions of A, B, and C which are close to the fracture limitation are crucial to the judgment of the propriety of forming, and since analysis result shows good agreement with the experiment result, numerical analysis has been adopted for determining the forming condition.

3.3 Study on optimum processing condition

Following the above, the influence that the loading path exerts on formability was studied through numerical analysis.¹¹⁾ Regarding determining the optimum loading path, it was found that the loading path indicated by the polygonal line graph in Fig. 13 was best.

Regarding the loading path and forming condition, expansion does not take place when only the internal pressure is being applied and until it reaches point a. Immediately after point a, expansion begins at the moment when the axial punch is loaded in addition to the internal pressure and proceeds in the section of a-b starting at the tube end. Thereafter, the expansion part of the blank tube comes in contact with the front edge of the movable dies. In the sections b-c-d, the movable dies with slits axially pushes the expansion part directly, and expansion progresses remarkably.

Next, the influence of the variation in loading paths on formability was studied through both numerical analysis and experiments. Under a constant counter load of $F = 38$ kN, the initial pressure p_1 , the intermediate pressure p_2 , and the final stage pressure p_3 were varied and well-formed samples could be obtained with the optimum loading paths. Buckling was developed under a pressure lower than the optimum level, while under a pressure above the optimum level, thickness reduction progressed on the side of the part expanded to the highest degree, resulting in fracture (Figs. 14, 15). These

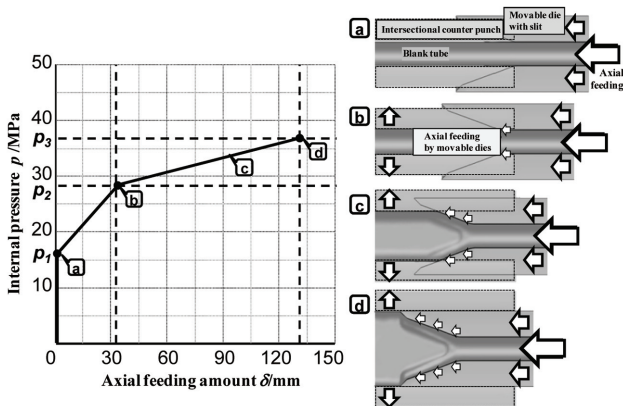
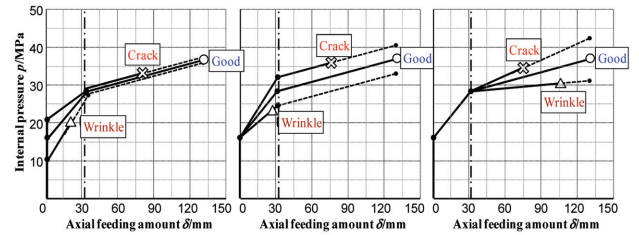


Fig. 13 Adequate loading path and forming conditions



(a)When p_1 is changed (b)When p_2 is changed (c)When p_3 is changed

Fig. 14 Various loading paths and formability

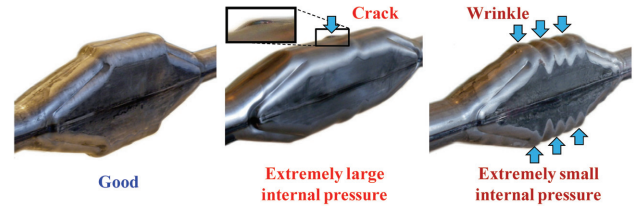


Fig. 15 Forming results when p_3 is changed

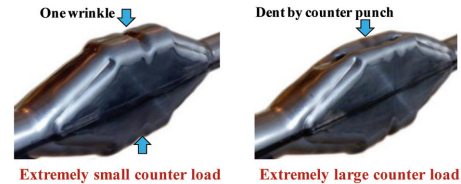


Fig. 16 Forming results when counter load is changed

results of numerical analysis and that of experiment showed good agreement.

Furthermore, in the abovementioned optimum loading path, effect of counter load on formability was studied by varying the counter load F . Under a counter load lower than the optimum counter load of $F = 38$ kN, a wrinkle developed in the neighborhood of the center in the longitudinal direction (Fig. 16). Thus, for expansion accompanied by axial feeding, the nearer a point is to the tube end, the higher the stress at the point in the axial direction, accordingly, expansion starts first at the tube end and proceeds and the blank tube deforms to a gourd-like shape. In this HF, deformation of the gourd-like shape is suppressed by the employment of counter punches installed to make the entire expansion part expand uniformly. However, in case of excessively low counter load, gourd-like type deformation progresses, causing a wrinkle in the center. On the other hand, in case of excessively high counter load, the counter punch sunk onto the formed sample and resulted in buckling.

3.4 Optimization of intermediate shape after the first hydroforming process

Next, with intent of determining the optimum intermediate shape after HF1, a forming analysis was conducted by varying the sectional figure of the expansion part.¹²⁾ The schematic sectional figure formed by HF1 is shown in Fig. 17. 0 mm, 5 mm, and 10 mm were taken for each amount of expansion in forward direction E_F and the amount of expansion in rearward direction E_R and six shapes by the combination thereof were prepared (Table 1). The expansion ratio was set at a constant value of $\eta = 2.4$ by adjusting the expansion height of E_{HF} .

The loading path is expressed by a polygonal line in the same

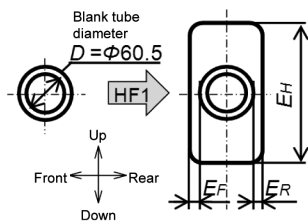


Fig. 17 Cross-sectional shape after HF1

Table 1 Trial conditions and thickness results of HF1

Sample No.	Front expansion size E_F (mm)	Rear expansion size E_R (mm)	Expansion height E_H (mm)	Thickness reduction rate ζ
0-0	0.0	0.0	173.0	0.20
0-5	0.0	5.0	168.0	0.32
0-10	0.0	10.0	163.0	0.36
5-5	5.0	5.0	163.0	0.30
5-10	5.0	10.0	158.0	0.32
10-10	10.0	10.0	153.0	0.37

way as in Fig. 13 and optimum condition was determined for each shape. The counter load was set at a constant value for each shape. On the basis of aforementioned conditions, the loading path and the counter load that enable forming without fracture were determined for each shape, and the strain distribution and thickness reduction ratio ζ after forming were studied. Here, thickness reduction ratio ζ is (thickness after expansion minus thickness of the blank tube) divided by the thickness of the blank tube. In addition, the estimated fracture limit was assumed as $\zeta = 0.4$ on the basis of past experimental data. The thickness distribution is shown in Fig. 18. Moreover, thickness reduction ratio ζ is shown in Table 1 together with other data.

Thickness reduction ratio ζ becomes highest at part A on the upper and lower end sides of the section of the expansion part in the center of the longitudinal direction. As for the samples of No.0-5, 0-10 and 5-10 that expand forward and backward unsymmetrically, the part A veers backward.

Furthermore, thickness reduction ratio ζ is smallest in No.0-0. For other samples, there is a tendency that buckling develops at part B where the shape expands frontward and backward, therefore, sufficient axial feeding cannot be rendered. However, in No.0-0, as there is no forward and backward expansion, part B does not exist; therefore, it is considered that sufficient axial feeding is possible. Furthermore, when samples of No.5-5 and No.0-10—where the expansion of total of 10 mm is applied in forward/backward directions—are compared, it is found that the thickness reduction ratio of the latter is higher, illustrating that the symmetrical shape is optimum.

Following the above, the strain path of the part A is shown in Fig. 19. It is found that as the amount of expansion in frontward and backward directions increases, the state of deformation transforms from pure shearing to uniaxial tension•two dimensional strain side, and thickness reduction proceeds.

From the above, in HF1—where the intersectional moving die technology is employed—it has become clear that well-formed samples can be obtained by selecting the optimum loading path on

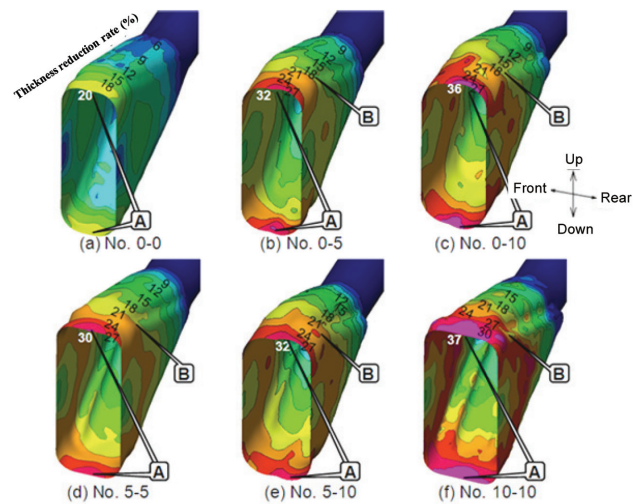


Fig. 18 Thickness contour of HF1

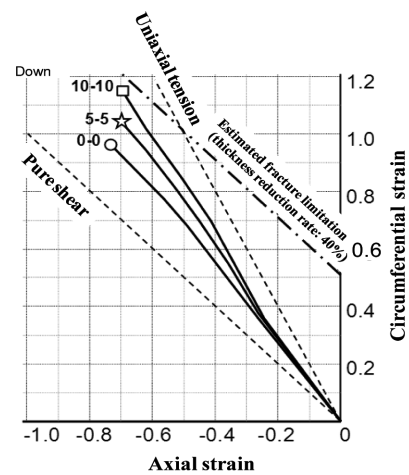


Fig. 19 Strain path of part A

the three axes of axial feeding, internal pressure, and counter load. Furthermore, regarding the intermediate shape after HF1, it has also been made clear that the symmetrical shape that expanded only along upward and downward directions is optimum.

4. Study on Detail of Second Hydroforming Process

Next, with the intent of determining optimum processing condition of HF2 and optimum intermediate shape after HF2, forming analysis was conducted by varying the cross-sectional shape after HF2 on the basis of No.0-0 after HF1.¹²⁾ Cross-sectional shape after forming in HF2 is shown in Fig. 20. Three different shapes were chosen by incorporating counterpunch vertical dimension C_H of 40 mm, 80 mm, and 120 mm (Table 2). The expansion ratio is 2.7 and constant.

The loading path was also expressed by a polygonal line as shown in Fig. 21, and the optimum condition of the axial feeding amount and the internal pressure at points (iv)•(v)•(vi) was selected for each shape. Among them, point (v) is the point where the material formed in HF1 is expanded and comes into complete contact with the movable dies and the counterpunches of HF2. Furthermore, the counter punches were position-controlled and the amount of

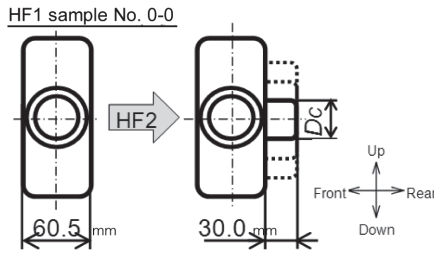


Fig. 20 Cross-sectional shape after HF2

Table 2 Trial conditions and thickness results of HF2

Sample No.	Counter punch height C_H (mm)	Thickness reduction rate ζ
0-0 . 40	40	0.22
0-0 . 80	80	0.29
0-0 . 120	120	0.39

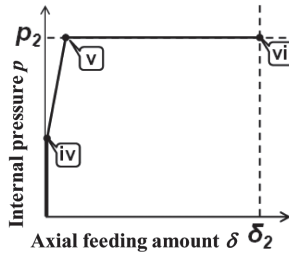


Fig. 21 Loading path of HF2

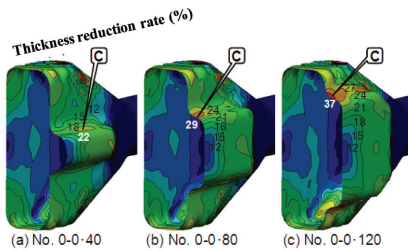


Fig. 22 Thickness contour of HF2

their travel was set at constant 30.0 mm. On the basis of abovementioned conditions, the loading path that enables forming without fracture was determined for each shape and the strain distribution and the thickness reduction ratio ζ were studied. The thickness distribution is shown in Fig. 22. Furthermore, the thickness reduction ratio ζ is shown in Table 2 together with other data.

It is found that the smaller the vertical dimension C_H of the counterpunch, the smaller the thickness reduction ratio. In HF2, the deformation of a part that corresponds to the vertical wall of the expanded part is large and there is a tendency of further progress in thickness reduction owing to lack of axial feeding.

Next, the thickness distribution of the cross-section at the center along the longitudinal direction is shown in Fig. 23. In the figure, the thickness distribution in HF1 is also shown together with. The part corresponding to the vertical dimension C_H of the counterpunch is also indicated in the figure with a line having an arrow on each end. From this, it is understood that the part where the thickness re-

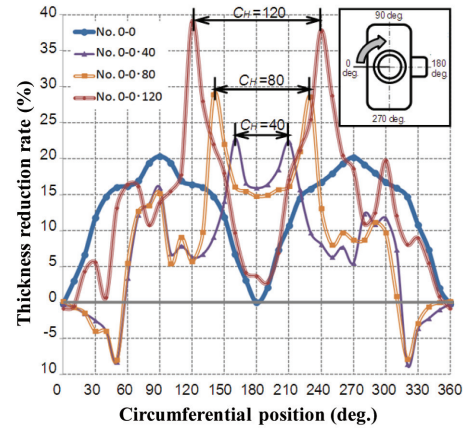


Fig. 23 Thickness distribution of HF2

duction reaches its peak corresponds to part C and it is considered that in case D_c is small, the part with small thickness reduction in HF1 comes to part C, however, in case D_c is large the part with large thickness reduction in HF1 comes to part C, and therefore, thickness reduction is localized.

From the abovementioned facts, it clear that well-formed samples can be obtained in HF2 through the optimum loading path and intermediate shape.

5. Trial Fabrication of Integrated One-piece Type Axle Housing

5.1 Result of trial fabrication of actual product

Finally, the actual fabrication of integrated one-piece type axle housing was attempted.⁹⁾ The processing step comprises three steps described in Fig. 5, and the processing conditions and the intermediate shapes in HF1 and HF2 were determined on the basis the detail study explained in chapters 3 and 4. Formability was repeatedly confirmed through FEM analysis, wherein the three processes were sequentially combined together and detailed forming condition, process, and die structure were studied, and then, trial of actual fabrication was conducted. Thus, a well-formed product, as shown, in Fig. 24 was obtained. The thickness reduction ratio ζ is 0.34.

From the above, it was verified that the fabrication of integrated one-piece type axle housing having a three dimensional curved surface is possible by the three HF processes of cold forming without intermediate heat treatment.

5.2 Characteristics of the trial product

In this study, upon the development of integrated one-piece type axle housing, a new product form was studied from the serious view point of weight-reduction without being prepossessed at all by the current product form.¹³⁾ The objectives of the new form to be realized by HF were the following: to enable weight reduction, to satisfy the parts performance of the current product, and to be formable in an integrated one-piece manner by HF. As for the parts performance, in addition to the rigidity and the fatigue resistance characteristics required for a suspension parts, vibration·sound characteristics was also taken into consideration, a requirement for a casing that incorporates differential gears which act as a vibration-causing source as well as being a sound emitting source.

The new form is of a three-dimensional smooth curved surface as shown in Fig. 4 which does not allow any stress concentration. Since there is no stress concentration in this form (Fig. 25), this form is advantageous not only in fatigue durability characteristics

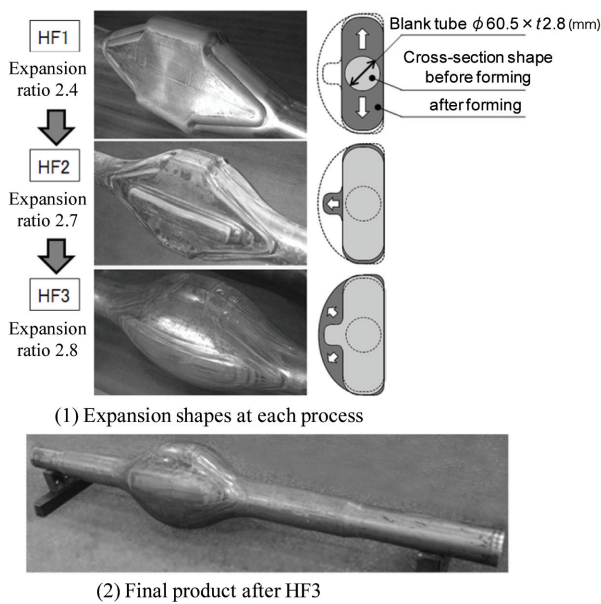


Fig. 24 Three-process hydroforming of integrated axle-housings with 3D curved shape

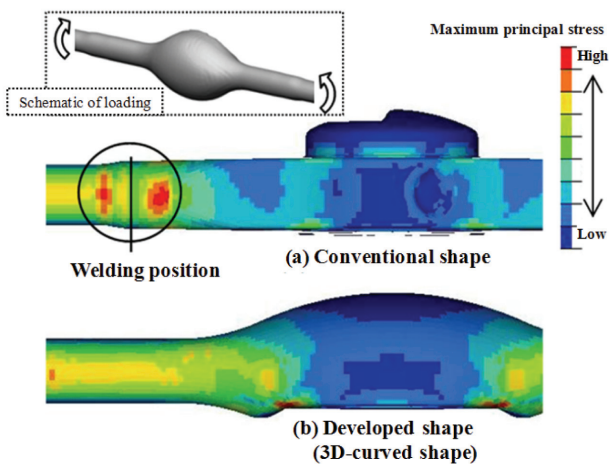


Fig. 25 Comparison of maximum principal stress contour between developed and conventional axle-housings on bottom surface (load direction: bump)

but also in vibration*sound characteristics as there is no flat portion. The side facing the body front has a flat part for installing differential gears; the surface around the flat part is also curved.

In order to confirm the fatigue durability characteristics of the trial product, brackets and other parts were fitted onto the aforementioned actual trial-produced axle, being made ready thereby for installation to an actual car (Fig. 26), vibration bench test was conducted in vertical direction and back and forth direction with respect to a car body. As the result, compliance with the desired fatigue durability characteristics and other parts characteristics has been confirmed. Furthermore, by eliminating welding, parts reliability has been enhanced and a weight reduction of approximately 10% has been obtained.¹⁴⁾

6. Conclusion

Aiming at enhancing the expansion ratio that used to be 1.0–1.4

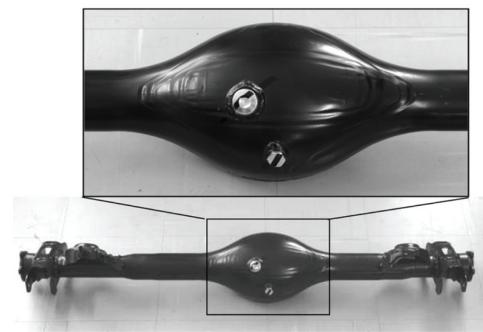


Fig. 26 Appearance of final prototype (to which vehicles can be attached)

in conventional HF, “multi-process unidirectional expansion process” that enables expansion with pure shearing deformation and “intersectional die technology” that enables sufficient axial feeding while suppressing buckling have been newly developed, and by applying the large expansion hydroforming technology developed by coupling the above process and the technology, innovative expansion ratio of 3.0 was achieved with cold forming process of HF without intermediate heat treatment.

In the intersectional movable die technology, control of axial feeding, internal pressure and counterpunch load on three axes is necessary, and the optimum loading path could be obtained by using numerical analysis. Furthermore, in the multi-process unidirectional expansion process, the optimum intermediate shape was made clear by fully utilizing the numerical analysis, and thereby large expansion hydroforming technology was established.

Furthermore, as the result of application of this technology to integrated forming of an axle housing, integrated forming without welding of a banjo-type axle housing that used to be comprise seven press-formed subparts welded together was realized and weight reduction as high as 10% was achieved.

With the use of the developed large expansion hydroforming technology, area of application of HF will be further expanded and further promotion of integrated forming of hollow parts, and weight-reduction is highly expected.

Reference

- 1) Manabe, K.: Journal of JSTP. 39 (453), 3 (1998)
- 2) Fuchizawa, S.: Journal of JSTP. 41 (478), 13 (2000)
- 3) Kuriyama, Y.: Journal of JSTP. 45 (524), 21 (2004)
- 4) Nasu, K.: 27th Metal Stamping Technology Seminar. 2000, p.1
- 5) Ueda, A., et al.: Journal of Press Working. 19 (9), 12 (1980)
- 6) Iridono, K., et al.: Jidosha Seibi No Kiso III Chassis. First Edition. Tokyo, Tokyo Denki Daigaku Shuppan Kyoku, 1991, p.46
- 7) Mori, S. et al.: Journal of JSTP. 29 (325), 131 (1988)
- 8) Mizumura, M., et al.: The Proceedings of the 2008 Japanese Spring Conference for the Technology of Plasticity. 2008, p.219
- 9) Wada, M., et al.: The Proceedings of the 62nd Japanese Joint Conference for the Technology of Plasticity. 2011, p.173
- 10) Sato, K., et al.: The Proceedings of the 2006 Japanese Spring Conference for the Technology of Plasticity. 2006, p.1
- 11) Wada, M., et al.: The Proceedings of the 2012 Japanese Spring Conference for the Technology of Plasticity. 2012, p.251
- 12) Wada, M., et al.: The Proceedings of the 2013 Japanese Spring Conference for the Technology of Plasticity. 2013, p.147
- 13) Kaneda, H., et al.: The Proceedings of the 62nd Japanese Joint Conference for the Technology of Plasticity. 2011, p.171
- 14) Kaneda, H., et al.: Journal of Society of Automotive Engineers of Japan. 67 (6), 90 (2013)

NIPPON STEEL & SUMITOMO METAL TECHNICAL REPORT No. 107 FEBRUARY 2015



Manabu WADA
Researcher, Dr.Eng.
Nagoya R&D Lab.
5-3 Tokaimachi, Tokai City, Aichi Pref. 476-8686



Keinosuke IGUCHI
Senior Researcher, Dr. Energy Science
Forming Technologies Research Lab.
Steel Research Laboratories



Masaaki MIZUMURA
Chief Researcher, Dr.Eng.
Forming Technologies Research Lab.
Steel Research Laboratories



Hiromitsu KANEDA
Technical Expert, Dr.Eng.
Component Engineering Development Dept.
Suzuki Motor Corporation